Letter to the Editor

Truncated disks – advective tori; new solutions of accretion flows around black holes

A. Hujeirat and M. Camenzind

Landessternwarte-Koenigstuhl, 69117 Heidelberg, Germany

Abstract. Our quasi-steady 2D numerical radiative hydrodynamical investigations of two-temperature accretion flows around black holes indicate that standard disks are thermally and hydrodynamically stable against transition to optically thin disks at large radii. Optically thin disks cool sufficiently rapid at large radii inducing a vertical collapse and forming thereby a standard disk which truncates close to the last stable orbit. In the absence of soft photons from the adjusting standard disk, we confirm the runaway cooling of the inner optically thin disk. This runaway however terminates if the radial flux of soft photons from the outer standard disk is taken into account. Instead, a cooling-driven front starts to propagates from outside-to-inside continuously extending the thick disk down to the very inner region where it terminates via an oppositely-oriented heating front that forms a hot advective and sub-keplerian torus.

The transition between the two configuration occurs where the ratio of the cooling to the heating time attains a minimum value. The transition is found to be rather sharp and gives rise to outwards-oriented motions of very hot plasma that enlarges the combined Compton-Synchrotron cooling regions considerably.

While the disk-torus configuration obtained depends weakly on whether the flow is a one or two-temperature plasma, one-temperature tori are hotter and fill larger volumes than their two-temperature counterparts.

Key words: black hole physics – accretion, accretion disks – hydrodynamics – radiation mechanisms: non-thermal

1. Introduction

Standard Shakura-Sunyaev disks (thereafter SSDs) should transit to optically thin disks (OTDs) close to the central accreting black hole to be consistent with observations (Blandford & Begelman 1998). Single and two-temperatures optically thin disks (Shapiro et al. 1975) are found to suffer of a thermal runaway instability (Piran 1978). Although this instability can be removed if advection is included (Narayan & Yi 1995), recent theoretical investigations indicate that the problem is at

least two-dimensional in nature and that one-dimensional treatments cannot recover consistently many important effects, like outflows, winds and convection (Abramowicz et al. 2000). Most importantly is that the nature and the location of, as well as the driver for the transition from SSDs to OTDs cannot be detected using 1D (Abramowicz et al. 2000) or self-similar treatment (Kato 1997).

It is commonly argued that transition occurs between 10^2–10^4 Schwarzschild radii ($R_S = 2GM/c^2$), and that disk-evaporation (Meyer & Meyer-Hofmeister 1994) and super-keplerian rotation might characterize the transition region (Abramowicz et al. 1998). In this letter we present new numerical results that reveal the nature of the transition region as well as the long time evolution of accretion disks around BHs using the robust implicit radiative hydrodynamical solver IRMHD2 (Hujeirat 1998).

2. Governing equations, initial and boundary conditions

Under axi-symmetry, the hydrodynamical equations consist of the continuity equation for the density, Euler's equations for three momenta, two equations for the internal energies of the ions and electrons, and one equation for the energy density of the radiation field. The equation of the radiative density is solved using the flux–limited diffusion (FLD) (Pomraning & Levermore 1981). The opacity κ is modified so that the radiation-matter collisional term $\Lambda_B \doteq \kappa\rho(T^4 - E)$ reduces to pure relativistic Bremsstrahlung $A\rho^2 T^{1/2} + B\rho^2 T$ in optically thin regions and to the radiative diffusion operator for higher optical depths. Here ρ, T and E denote the density, temperature, density of radiation and A and B are constant coefficients.

For incorporating synchrotron cooling Λ_{Syn}, we assume the magnetic pressure to equalize the turbulent pressure, and use the relation $\Lambda_{\mathrm{Syn}} = (E_{\mathrm{mag}}/E)\Lambda_C$, where E_{mag} and E denote the magnetic and photon energies, and $\Lambda_C = A\rho(T_e - T_{\mathrm{rad}}) \times (1 + \frac{4kT}{m_e c^2})E$ is the Compton cooling function (Rybiki & Lightman 1979). Combining both processes, we end up with the modified Compton cooling function:

$$\Lambda_{\mathrm{Compt}}^{\mathrm{mod}} = \left(1 + \frac{\alpha^2 P_e}{2\,E}\right)\Lambda_C, \tag{1}$$

where α and P_e denote the turbulent viscosity coefficient and the electron- pressure, respectively.

Gravity of the central object is described in terms of the quasi–newtonian potential of Paczynski & Wiita (1980). In all models, we assume a $10\,M_\odot$ central black hole, and an accretion rate of $-\dot{\mathcal{M}} = 10^{17}\mathrm{g\,s^{-1}}$ is set to enter the domain $D = [0 \le \theta \le \pi/2] \times [1 \le r \le 10]$ via a thin disk across the outer boundary. The accretion flow will be followed down to some radius within the marginal stable orbit, where GR–effects become important. We have set this inner radius as $R_{\mathrm{in}} = 2.75\,R_{\mathrm{S}}$. All radii are given in the following in units of R_{in}.

Although the solutions sought are initial-conditions-independent, we mention them here for completeness. We split D into the disk region $D_{\mathrm{disk}} = [0 \le \theta \le \theta_{\mathrm{d}}] \times [1 \le r \le 10]$ and a corona region $D_{\mathrm{C}} = D - D_{\mathrm{disk}}$, where $\theta_{\mathrm{d}} = H/r$ and H denotes the classical thickness of the disk.

In D_{disk} the matter is set to rotate keplerian with $\Omega_{\mathrm{K}}(r,\theta) = GM/r(r - R_{\mathrm{S}})$, and we set the density $\rho(r,\theta) = \rho(10,\theta) = \rho_0 \times max(\mathrm{e}^{-(z/H)^2}, 10^{-4})$ and $\mathrm{T}(r,\theta) = \mathrm{T}(10,\theta) = \mathrm{T}_0$, where $dz = r\,d\theta$ and the subscript '0' denotes the corresponding equatorial value at the outer boundary. In D_{C} we set $\Omega = 0$, $\rho(r,\theta) = 10^{-4}\,\rho_0$, $\mathrm{T}(r,\theta) = \mathrm{T}_{\mathrm{Virial}}$. The poloidal component of the velocity field in D is set to vanish.

Since we are interested in steady configurations and since the flow is viscous and ρ in D_{C} is not sufficiently small, we have found that an unreasonably large shear ($\partial V/\partial \theta$) along the inner boundary shows up whenever a non-rotating cold corona is considered. Therefore, the actual advantage of incorporating a corona is to reduce the shear and to keep the Mach numbers along R_{in} comparable.

Across the inner boundary, free-fall for the radial velocity and stress–free conditions for the angular velocity are imposed. Normal symmetry and anti–symmetry conditions are assumed along the equator and along the polar axis. The domain of integration is divided into 200×70 strongly stretched finite volume cells in the radial and vertical directions, respectively.

Following Shapiro et al. (1975, SLE), the ions are heated via turbulent dissipation and the electrons cool via Bremsstrahlung and comptonization, where the disk is the only source of soft photons. For dynamical viscosity we use $\eta_{\mathrm{t}} = \rho\nu_{\mathrm{t}} = \rho\alpha\,V_{\mathrm{S}}H$ as the turbulent diffusion coefficient, where $H = 0.1r$ and $\alpha = 0.1$ are used.

The calculations proceed as follows. Using the above-mentioned initial conditions we have carried the calculations till the maximum time-independent residual Res_2 has dropped below a certain small value ϵ_{c}. We stress here that what characterizes the steadiness of our solutions is $Res_2 \le \epsilon_{\mathrm{c}}$ and not the number of orbital periods.

3. Truncated disks – advective tori solutions

Let r_{tr} be the transition radius between an SSD and an inner OTD, and assume the effective gravity g_{eff} at $r_- = r_{\mathrm{tr}}(-\epsilon)$ is comparable to that at $r_+ = r_{\mathrm{tr}}(1+\epsilon)$ for a given small ϵ. Since
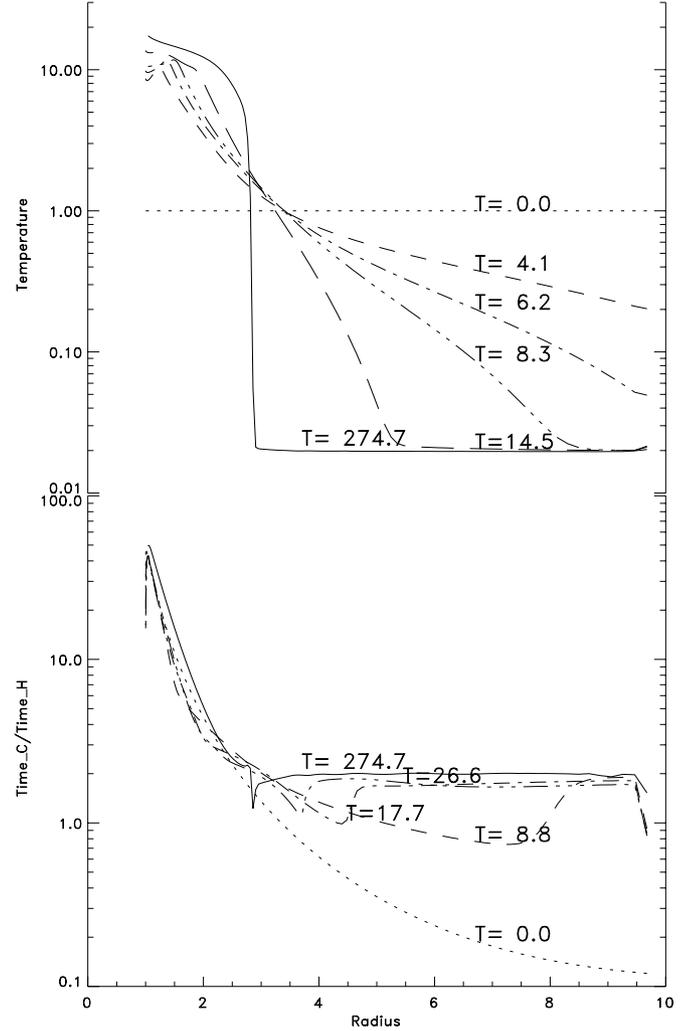

Fig. 1. Synchrotron-2T model. The profiles of the electron temperature (top, Temperature in units of 5×10^7 K) and the ratio of the cooling time to the heating time $\tau_{\mathrm{C}}/\tau_{\mathrm{H}}$ at different time levels T (in units of the orbital periods at R_{S}) are shown. In this model a material flux $\dot{\mathcal{M}} = 2 \times 10^{16}\,\mathrm{g\,s^{-1}}$ is set to enter the domain of integration through the outer boundary. Note the rapid steepening of the electron temperature around the point where $\tau_{\mathrm{C}}/\tau_{\mathrm{H}}$ is minimum.

the radiative density $E^- = E(r = r_-) < E^+$, the ratio of the cooling time to the heating time at r_- is roughly $\tau_{\mathrm{C}}/\tau_{\mathrm{H}} \sim \alpha D^2 T^{1/2}/(\rho\Omega)$, where $D^2 = (r\partial\Omega/\partial r)^2 + (\partial\Omega/\partial\theta)^2$. Moreover, requiring the transition to be smooth, standard disk theory predicts that $\tau_{\mathrm{C}}/\tau_{\mathrm{H}}(r = r_{\mathrm{tr}}) \approx \alpha$ which coincides with the initial profile in Fig. 1. Thus, the ratio $\tau_{\mathrm{C}}/\tau_{\mathrm{H}}$ corresponding to the outermost annuli of an OTD is smaller than one and therefore the gas starts to cool rapidly initiating thereby a considerable vertical motion that enhances density condensations along the equator. The gas-temperature at r_- reaches the minimum radiative temperature T_{rad}^-. In the absence of external input of energy, E attains a maximum at r_{tr} and therefore transporting an inwards-directed radiative flux $F_{\mathrm{rad}}^{\mathrm{r}} = \frac{\lambda}{\chi} \times \partial E/\partial r$, where λ is the radiative-flux-limiter, $\chi = \rho(\kappa + \sigma)$ and σ denotes the
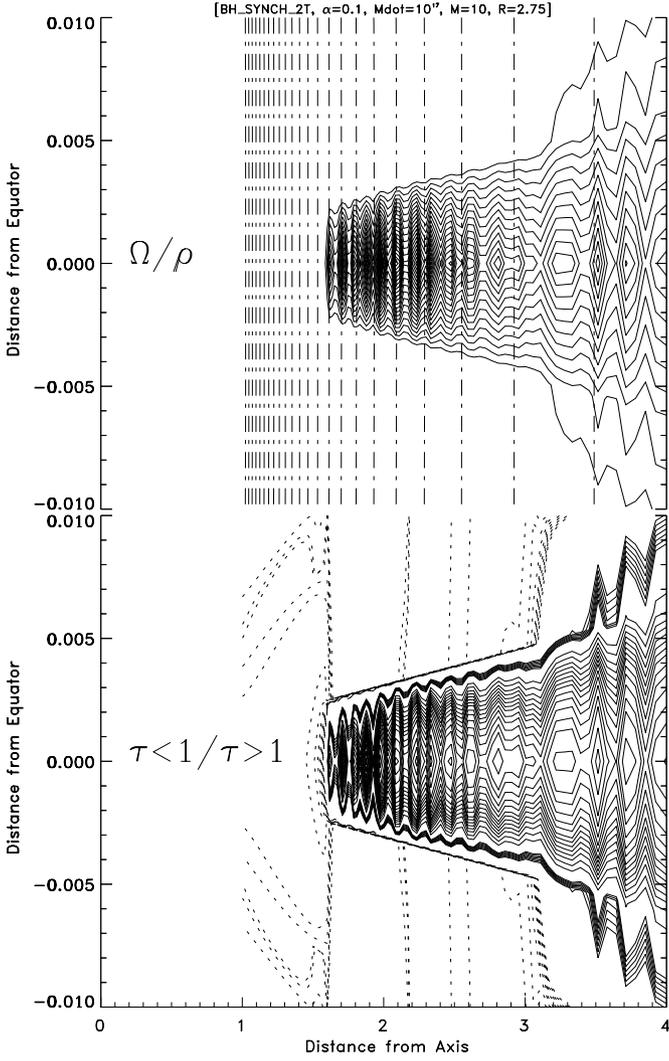
Fig. 2. Synchrotron-2T model. 25 equi–distant contour–lines of density ρ and angular velocity Ω (solid and dashed lines, top), and of the modified optical thickness τ_{mod} (bottom; contours with $\tau > 1$ are plotted with solid lines and $\tau < 1$ with dotted lines) of the media in the disk around $10\,M_\odot$ after 2000 orbital periods (in units of the orbital period of the marginal stable orbit). A material flux $\dot{\mathcal{M}} = 10^{17}\,\mathrm{g\,s^{-1}}$ is set to enter the domain of integration through the outer boundary. The distances from the axis and the equator are in units of $2.75\,R_\mathrm{S}$. In this model cooling via relativistic Bremsstrahlung, Compton and synchrotron are incorporated. Note the disk truncation around the transition radius $r_{\mathrm{tr}} = 1.65$
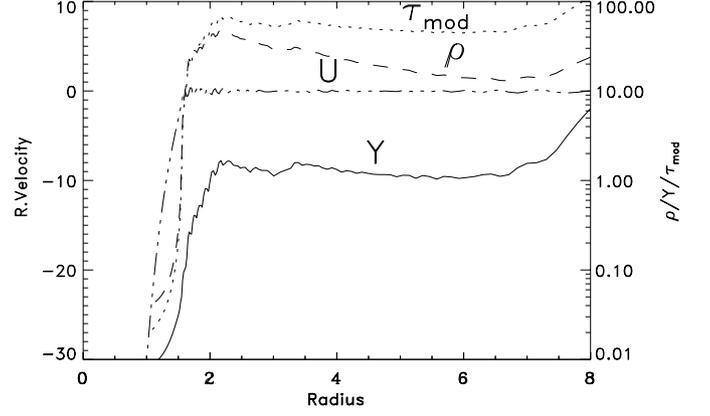

Fig. 3. Synchrotron-2T model. The profiles of the radial velocity U (left axis in $8.3 \times 10^7\,\mathrm{cm\,s^{-1}}$ units), density ρ in $1.45 \times 10^{-6}\mathrm{gr/cm^3}$, modified optical depth τ_{mod} and Compton Y parameter (right axis) along the equator. Note the rapid acceleration and the strong decrease of the variable-values in the torus.
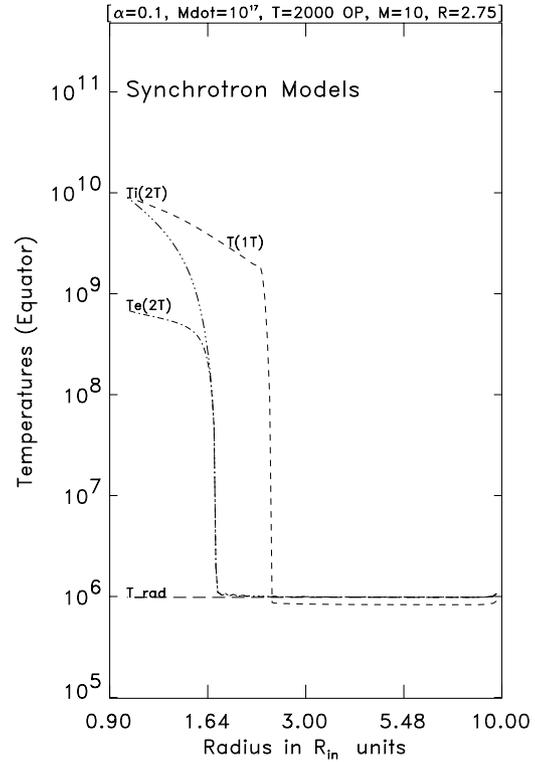

Fig. 4. The profiles of the temperatures along the equator. $T(1T)$ correspond to the gas temperature obtained using the single-temperature description. $T_\mathrm{e}(2T)$ and $T_\mathrm{i}(2T)$ correspond to the electron- and ion-temperature obtained using the two-temperature description. T_rad is the effective radiative temperature. In these two models cooling via Bremsstrahlung, Compton and synchrotron cooling have been incorporated.

scattering coefficient. This implies that the gas at r_+ will cool to T_{rad}^- also.

We note that $F_{\mathrm{rad}}^{\mathrm{r}}$ at r_{tr} is even comparable to the vertical flux $F_{\mathrm{rad}}^{\mathrm{z}}(r_+) = \frac{\lambda}{r\,\chi} \times \partial E/\partial\theta|_{r=r_+}$, implying that a considerable flux of soft photons goes into the OTD maintaining $T \geq T_{\mathrm{rad}}^-$. Our calculations show that T_{rad}^- is of the order of $(H/r) \times T_{\mathrm{rad}}^+$, therefore terminating the so called runaway cooling of the gas at r_- (Piran 1978). Since $\tau_\mathrm{C}/\tau_\mathrm{H}$ is small at the largest radii, the 'limited' runaway cooling acquire the form of

a cooling front which starts propagating from outside-to-inside forming behind its front an SSD with $\tau_\mathrm{C}/\tau_\mathrm{H} \geq 1$.

Consequently, as our calculations indicate also, the transition from SSDs to OTDs is thermally unstable. The transition
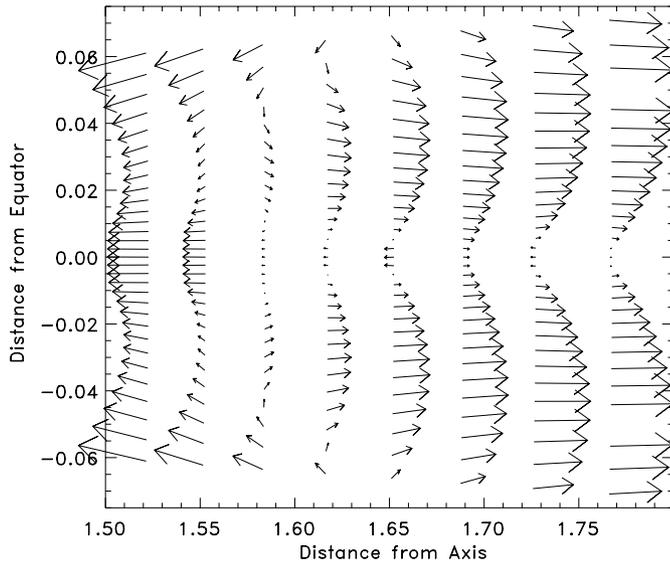
LETTER

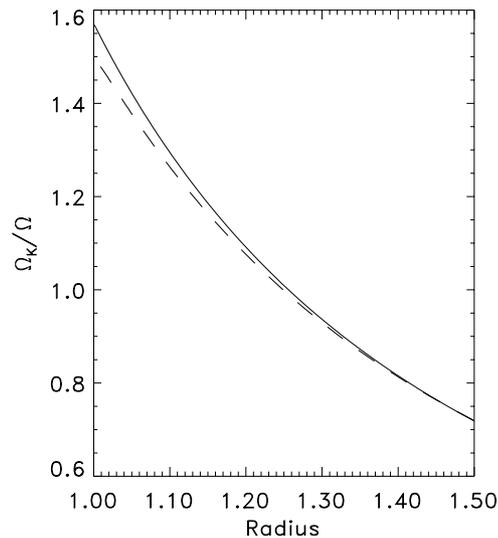**Fig. 5.** Synchrotron-2T model. The velocity field around the transition radius.

Fig. 6. Synchrotron-2T model. The profile of the angular velocity along the equator (dashed line) to be compared to the actual keplerian velocity (solid line) in the torus.

is hydrodynamically unstable also because $g_{\rm eff}$ at $r_{\pm}$ are negligibly small, otherwise super-keplerian rotation is required (see Abramowicz et al. 1998).

When and where does transition occur?

The calculations confirm that those annuli with $\tau_{\rm C}/\tau_{\rm H} \leq 1$ are thermally unstable and undergo a rapid vertical contraction associated with fluid motion to end up with a stable configuration characterized by $\tau_{\rm C}/\tau_{\rm H} \geq 1$ (Fig. 1).

On the other hand, close to the last stable orbit, $g_{\rm eff}$ becomes significant and induces a strong inwards acceleration of the matter and therefore a rapid density-decrease. Since the heating time scale is density-independent and increases with decreasing radius, a heating front forms right at the inner boundary and starts propagating outwards forming behind its front a hot advective sub-keplerian rotating torus characterized by a relatively large $\tau_{\rm C}/\tau_{\rm H}$ (see Fig. 1, 4 and 6). The front terminates at a critical radius where $\tau_{\rm C}/\tau_{\rm H}$ attains a minimum value. Unlike transitions at large radii, the rapid density-decrease here is stable as the different time scales involved are comparable and a further density enhancement via vertical (dynamical) contractions will be canceled immediately by a further inwards acceleration of the matter. The strong increase of temperature at $r_{\rm tr}$ is therefore necessary to maintain a rapid viscous transport of angular momentum outwards.

As our results show, the torus-volume is relatively small to produce the required emission of comptonized photons to be consistent with observation. However, we find that the strong increase of the ion-pressure at $r_{\rm tr}$ induce outwards motions of hot electrons that sandwiching the cool disk from both sides (Fig. 5). The resulting configuration is then sufficiently large for inversely comptonizing the flow of the hot electrons so that the spectrum is likely to correspond to a hot state with a significant black-body emmision in the background.

Combining these with our previous results (Hujeirat & Camenzind 2000), we conclude that configurations of truncated standard disks in the outer region and formation of hot ion tori in the inner region may occur for a large variety of accretion rates and turbulent viscosity coefficients.

References

Abramowicz, M., Igumenshchev, I.V., Lasota, J-P, 1998, MNRAS, 293, 443

Abramowicz, M., Björnsson, G., Igumenshchev, I., 2000, PASJ, 52, 295

Blandford, R., Begelman, M.C, 1999, MNRAS, 303, L1

Hujeirat, A., 1998, MNRAS, 298, 320

Hujeirat, A., Camenzind, M., 2000, A&A, in press

Kato, S., 1997, PASJ, 49, 503

Meyer, F., Liu, B.F., Meyer-Hofmeister, 2000, Astro-ph/0002053

Narayan, R., Yi, I., 1994, ApJ, 428, L13

Piran, T., 1978, ApJ, 221, 652

Pomraning, G.C, Levermore, C.D., 1981, ApJ, 248, 321

Paczynski, B., Wiita, P.J., 1980, A&A, 88, 23

Shapiro, S.L., Lightman A.P., Eardley, D.M., 1976, ApJ, 204, 187 (SLE) 1982, Nat, 295, 17